Journal of Cleaner Production 171 (2018) 884–891

Contents lists available at ScienceDirect

Journal of Cleaner Production

journal homepage: www.elsevier.com/locate/jclepro

Fractal-like concepts for evaluation of toxic metals adsorption efficiency of feldspar-biomass composites

Bamidele I. Olu-Owolabi [a], Paul N. Diagboya [b, *], Emmanuel I. Unuabonah [c], Alimoh H. Alabi [a], Rolf-Alexander Düring [d], Kayode O. Adebowale [a]

[a] Department of Chemistry, University of Ibadan, Ibadan, Nigeria
[b] Department of Chemistry, Vaal University of Technology, Vanderbijlpark, Guateng, South Africa
[c] Department of Chemical Sciences, Redeemer's University, Ogun State, Nigeria
[d] Institute of Soil Science and Soil Conservation, Justus Liebig University, Giessen, Germany

ARTICLE INFO

Article history:
Received 3 April 2017
Received in revised form
6 October 2017
Accepted 8 October 2017
Available online 10 October 2017

Keywords:
Carica papaya seed
Pine cone
Clay-biomass composite
Fractal pseudo-second order model
Brouers-Sotolongo adsorption isotherm model

ABSTRACT

Effective treatment of metals polluted water may be achieved using low-cost materials synergistically modified to obtain composite adsorbents. Thus, feldspar–biomass composites have been prepared via calcination of feldspar (FLC) and *Carica papaya* seeds or pine cone seeds to yield *Carica papaya*-FLC (CPF) and pine-cone-FLC (PCF) composite adsorbents, respectively. The composites physicochemical properties and effectiveness for Pb(II), Cd(II) and Cu(II) removal in aqueous solutions were examined. Results showed that calcination did not promote any structural modification in the basic FLC lattice. Though CPF and PCF exhibited lower specific surface area when compared with the FLC, their cation exchange capacities were enhanced. Unlike on the FLC, the metals adsorption on CPF and PCF were higher (>40%) for Cu(II) and Cd(II), pH independent and faster. The study showed that adsorption process on a system with varying types of surface sites and with varying affinity for an adsorbent can best be described by the fractal-like kinetic and equilibrium adsorption isotherm models (fractal pseudo-second order kinetic model and fractal Brouers–Sotolongo adsorption model) compared with the classical models (pseudo-first order and pseudo-second order kinetic models, Langmuir and Freundlich adsorption isotherm models). These adsorption processes were thermodynamically spontaneous, feasible and endothermic; however the modification significantly reduced their energy requirements. The Brouers–Sotolongo model showed that modification of FLC increased the width of the sorption energy distribution on the composites indicating the heterogeneity of the surface adsorption sites. Though no single classical theory of sorption can presently be put forward to explain the overall adsorptive process, metals adsorption on these feldspar-biomass composites are heterogeneous and complex processes with fractal architecture.

1. Introduction

The challenges of water polluted by toxic chemical substances are ubiquitous and enormous; it has been reported that over one billion people lack reliable access to clean water and 2.3 billion people of the global population live in water-stressed areas, a number that will increase by 52 percent in 2025 (Diagboya et al., 2016; Okoli et al., 2017; Mokwenye et al., 2016). Of the several methods employed for water treatment such as filtration, membrane technology, ion exchange, reverse osmosis, electrochemical treatment, evaporation recovery, and sorption processes, sorption-based methods have proven to be of priority due to several associated technological, economical and environmental benefits, such as low cost of materials and processing, available in abundance, high efficiency of sorption and environmental friendliness (Olu-Owolabi et al., 2017). Synergistic combination of low cost adsorbents (Unuabonah et al., 2013a; Olu-Owolabi et al., 2016a, 2017) is a recent breakthrough in adsorption science. This has enabled abundant low cost materials which hitherto had one or more drawbacks for sorption applications to be made beneficial through synergistic combination of their useful properties in the composites. These combinations have led to better adsorbent properties such as high cation exchange capacity (CEC), reduced/eliminated bleeding, enhanced mechanical strength, pore size, better stability

* Corresponding author.
E-mail address: pauldn2@yahoo.com (P.N. Diagboya).

https://doi.org/10.1016/j.jclepro.2017.10.079
0959-6526/

and durability, re-usability, sometimes larger surface area, and consequently higher sorption efficiency (Unuabonah et al., 2013a; Olu-Owolabi et al., 2016a, 2017).

In describing the sorption processes occurring in adsorbent materials, the simplistic diffusion equations are commonly used: the Lagergren (1898) Pseudo-First Order (PFOM) and Pseudo-Second Order (PSOM) equations, Langmuir and Freundlich equations. However, these equations do not take into consideration the complex nature of sorbents and its effects on the kinetics of sorbates. Apart from the sorbent's fractal surfaces (boundaries separating mass and pore spaces), several physical properties depend on the scaling behaviour of the entire sorbent mass and entire pore spaces (Gaspard et al., 2006). The homogeneous Fractal Pseudo-Second Order Model (FPSOM) and Brouers–Sotolongo model takes into consideration the various fractal dimensions such as the pore fractal, the surface fractal and the mass fractal (Altenor et al., 2009; Haerifar and Azizian, 2014). Indeed application of these fractal models present many advantages with regard to other more classical kinetic models. For instance, the equation can be used to derive the fractional time (α) index which is an important factor that has influence on the adsorption properties of the adsorbent. A major advantage is that the fractal kinetic and isothermal analysis can be used to characterize irregular sorbents by taking into consideration the different fractal dimensions. Of the various fractal analysis, the methods based on analysis of adsorption isotherm play an important role since they require only one complete adsorption isotherm for a given adsorbent to calculate the surface fractal dimension (Gaspard et al., 2006).

Though we have initially developed a modified feldspar adsorbent from a combination of sulphuric acid, aniline, polyvinyl alcohol and feldspar (SAPK) which gave better sorption properties for the removal of Pb(II), Cd(II) and Zn(II) from aqueous solution when compared with pristine feldspar (Unuabonah et al., 2013b), the aim of this study was to develops more efficient composite adsorbents from calcined feldspar and two separate biomasses (*Carica papaya* or pine cone seeds) for the removal of Pb(II), Cd(II) and Cu(II) ions. The kinetic and equilibrium sorption data will then be described by comparing the classical diffusion and fractal adsorption models.

2. Materials and method

2.1. Biomass and clay pretreatments, composites preparations and characterizations

The *Carica papaya* and pine cone seeds were sourced from local markets in Ibadan and the University of Ibadan, Botanical garden, respectively. The seeds were washed and dried at 105 °C to remove moisture. These were then separately pulverized to fineness using a steel blender, sieved through 230 μm mesh size, and stored in air-tight containers. Feldspar (FLC) was washed and subsequently treated to remove organic matter using hydrogen peroxide (Diagboya et al., 2015). The FLC sample was then oven dried at 105 °C, cooled, ground, and sieved (230 μm mesh) (Supplementary Material –SM 1.1).

Equal masses of FLC sample and either of the *Carica papaya* or pine cone samples were mixed with 0.1 M NaOH solution. The mixtures were heated to dryness, calcined and washed to remove residual NaOH. The products were subsequently oven dried at 105 °C. The purified Feldspar, *Carica papaya* and pine cone seeds modified feldspar were thereafter referred to as FLC, CPF and PCF adsorbents respectively (Fig. 1; SM 1.2).

The FLC, CPF and PCF samples were characterized by determining their pH in water, pH at point zero charge (pHpzc) by the solid addition method, *X*-ray diffractograms using Bruker Phaser Diffractometer scanning from 5 to 70° 2-theta, infra red spectra using Fourier transform infrared (FTIR) spectrometer (Perkin Elmer Instruments Co. Ltd., USA), Cation Exchange Capacity (CEC) using the sodium saturation method (Olu-Owolabi et al., 2016a), and surface area using Micromeritics ASAP 2020 M + C accelerated surface area analyzer (Micromeritics Instrument Corporation, USA) (SM 1.3).

2.2. Adsorption experiments

Analytical grade Pb(II), Cu(II), and Cd(II) salts were prepared from their chloride salts (Merck, Germany). Adsorption experiments were then carried out by adding 20 mL solution of specified concentration of any of the metals above into vials containing 100 mg of the adsorbent. The adsorbent and metal ion mixtures were then equilibrated at 100 rpm at 25 °C on an orbital shaker. When necessary pH of working solutions were adjusted by adding drops of either 0.1 M HCl or NaOH. Preliminary experiment on the effect of pH on metals' adsorption was carried out by varying pH from 2.0 to 7.0 using 50 mg/L of metal ions and equilibrating for 1440 min. Effect of time was examined by using 50 mg/L of the metal ions and time varied from 15 to 1440 min. Equilibrium experiments were carried out at temperatures of 25 and 50 °C, while varying the concentrations (0–80 mg/L) at solution pH of 5.5 ± 0.2 and equilibrating time of 1440 min. At equilibrium, the vials are centrifuged at 3000 rpm for 10 min, and the concentrations of metal ions remaining in solution were determined using the Varian AA240FS Atomic Absorption Spectrometer (AAS). All experiments were duplicated and mean values were used for computation.

The reusability study was carried out using 0.1 g of the metal-loaded composites. The adsorbed metal ions were desorbed by shaking in 20 mL of 0.5 M HCl twice at 200 rpm for 30 min and then ultra-pure water (same speed and time) before reuse. A solution of 20 mL of 80 mg/L of each metal ion was employed during the batch reusability study at incubation time of 180 min. and room temperature. Subsequently, the mixture was centrifuged at 4000 rpm and the supernatant was read to determine the amount of metal ion left in solution. This procedure was repeated thrice.

2.3. Data analysis

The initial (C_o) and final (C_e) metal ions concentrations in solutions were used to calculate the amounts of metal ions adsorbed – q_e (mg/g) using equation (1):

$$q_e = (C_o - C_e)V/m \tag{1}$$

where V and m are the volume of the solution (mL) and mass (g) of adsorbent used, respectively.

The Lagergren (1898) Pseudo-First Order (PFOM) (equation (2)) and Pseudo-Second Order (PSOM) (equation (3)) kinetics models, and the homogeneous Fractal Pseudo-Second Order Model (FPSOM) (Haerifar and Azizian, 2014) (equation (4)) were used to describe the experimental data.

$$\log(q_e - q_t) = \log q_e - (k_1 t)/2.303 \tag{2}$$

$$t/q_t = 1\Big/\left(k_2 q_e^2\right) + t/(q_e) \tag{3}$$

$$q_t = \frac{k_f q_e^2 t^{\alpha}}{1 + k_f q_e t^{\alpha}} \tag{4}$$

where q_e and q_t are amount adsorbed (mg g^{-1}) at equilibrium and time t, respectively; and k_1 (min^{-1}) and k_2(g ìg^{-1}min^{-1}) are the rate

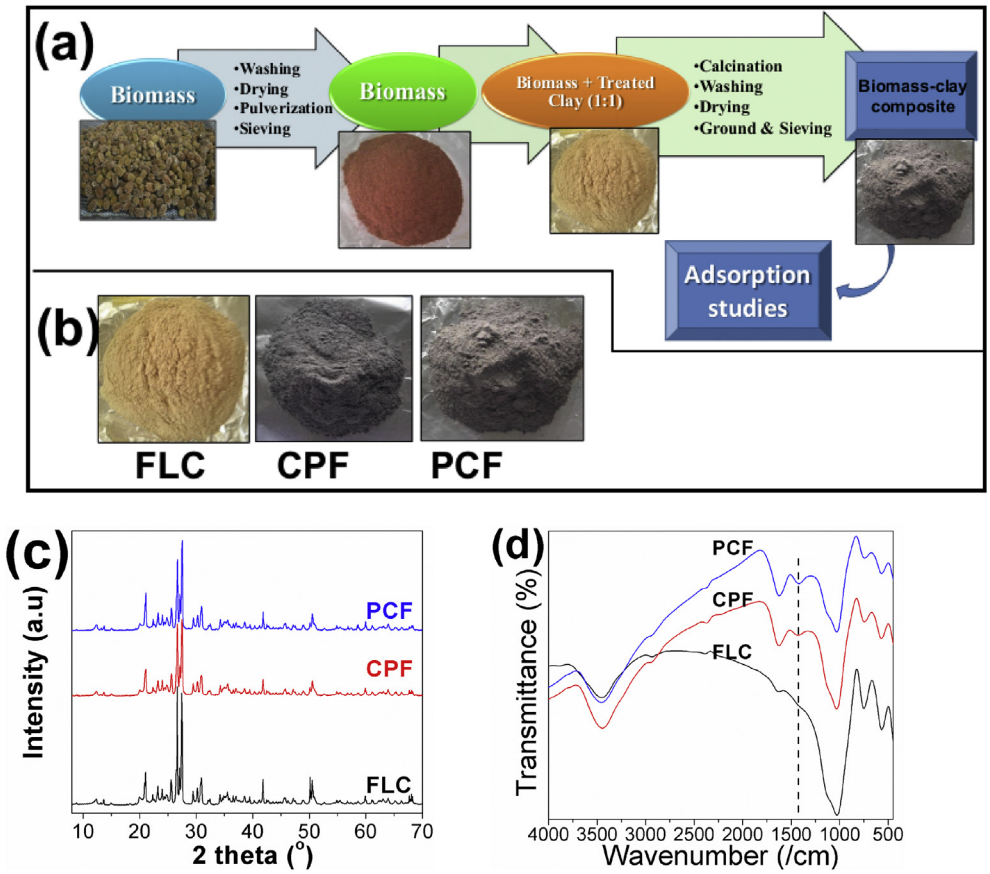

Fig. 1. (a) Schematics of composites preparation; (b) FLC, CPF and PCF adsorbents before adsorption; (c) *X*-ray diffraction patterns of the adsorbents; (d) FTIR spectra of the adsorbents.

constants of the PFO and PSO, respectively. The α is the fractional time index and k_f(g mg^{-1}min^{-1}) are the rate constants of the FPSOM. The q_e and rate constants were obtained using the KyPlot software.

Thermodynamic parameters were determined using the equilibrium constant (equation (5)) where b is the Langmuir constant. The enthalpy of adsorption (ΔH°) of the metal ions onto the various adsorbents was determined using the Van't Hoff (equation (6)). The Gibbs free energy (ΔG°) data was determined using equation (7).

$$K = b \tag{5}$$

$$\ln\left(\frac{K_{T1}}{K_{T2}}\right) = \frac{\Delta H^\circ}{R}\left(\frac{1}{T_1} - \frac{1}{T_2}\right) \tag{6}$$

$$\Delta G^o = -RT\ln(b) \tag{7}$$

According to Milonjic (2007), *b is* given in dm^3 mol^{-1}, then *K* can be easily recalculated as dimensionless by multiplying it by 55.5 (number of moles of water per liter of solution). Hence, the correct ΔG° value can be obtained from equation (8).

$$\Delta G^o = -RT\ln(55.5{*}1000{*}b) \tag{8}$$

The term 55.5*K* (dm^3 mol^{-1} mol dm^{-3}) is dimensionless. In the case when *K* is given in dm^3 g^{-1}. Similarly, *b* can be easily recalculated to become dimensionless by multiplying it by 1000 [1 dm^3 = 1000 mL (or g, since solution density is ≈ 1 g mL^{-1})], where *b* is the Langmuir parameter. ΔS° is obtained from equation (9).

$$\Delta G^o = \Delta H^o - T\Delta S^o \tag{9}$$

The nonlinear forms of the Langmuir (1916) model (equation (10)), Freundlich (1906) model (equation (11)) and Brouers–Sotolongo model (fractal model for modeling equilibrium data) by Gregg and Sing (1967) often referred to as BSM (equation (12)) were employed in describing the adsorption process.

$$q_e = \frac{Q_O b C_e}{1 + bC_e} \tag{10}$$

$$q_e = k_f C_e^n \tag{11}$$

$$Q_e = Q_{\max}(1 - (\exp(-K_w C_e^\alpha)) \tag{12}$$

where Q_o is the maximum adsorption capacity per unit weight of adsorbent, *b* is a solute–surface interaction energy-related parameter, q_e and C_e are same as above, k_f and *n* are the Freundlich model capacity factor and the isotherm linearity parameter, respectively. The BSM constants Q_{max} is the saturation value, $K_w = k_f/Q_{max}$ where k_f is the low C_e (SM 1.4).

3. Results and discussion

3.1. Physicochemical characterizations and preliminary result of effect of pH on adsorption

Results of the physicochemical parameters are shown in

Table 1
Physicochemical parameters of FLC, CPF and PCF.

	pH in H_2O	pH in KCl	CEC (meq/100 g)	pHpzc	Surface area ($m^2\ g^{-1}$)
*PC	4.8	4.4	125.7	5.0	–
*CP	5.6	5.3	194.8	5.3	–
FLC	7.4	6.8	27.9	7.1	15.0
CPF	9.2	8.2	37.2	8.1	5.5
PCF	8.0	6.8	40.0	7.3	8.9

*PC – Pine cone; CP – *Carica Papaya;* CEC – cation exchange capacity; pHpzc – pH at point of zero charge.

Fig. 1c–*d* and Table 1. The results indicate that the composite adsorbents– CPF and PCF adsorbents exhibited lower specific surface area (SSA) of 5.5 and 8.9 $m^2\ g^{-1}$ when compared with the FLC (15 $m^2\ g^{-1}$). This indicated that calcination of FLC with the biomasses resulted in the blockage of some pore spaces in the FLC leading to the reduction in the composites' SSA. In contrast to the SSA, CEC of composites were higher than that of FLC; suggesting enhancements in the metals' adsorption capacities of the composites. Olu-Owolabi et al. (2016a; 2017) have reported similar results for SSA and CEC in bentonite and kaolinite clays. The pH and pHpzc values of the composites were higher than those of the biomasses and FLC. Both values were slightly increased in PCF but higher in CPF. These increases in pHpzc values for CPF and PCF suggested that the modification process resulted in the formation of ionizable surface oxygen groups which can contribute delocalized π–electrons during the adsorption process because of the presence of functional groups such as pyrones or chromenes (Rivera-Utrilla and Sanchez-Polo, 2003; Unuabonah et al., 2013a). The powder XRD diffraction patterns of FLC, CPF and PCF (Fig. 1c) showed that both CPF and PCF exhibited the typical diffraction pattern of FLC. The reflections at 21° (2θ) ($2\overline{0}1$) and 27.80° (2θ) (040) can be assigned to microcline and feldspar minerals, respectively. The reflections at 25.9° (2θ) (002) and 30.44° (2θ) ($1\overline{3}1$) suggests that the crystals of the feldspar sample used in this study were partly monoclinic and partly triclinic. The reflection at 26.60° (2θ) is indicative of quartz (131), which is present in the raw material. The diffraction patterns of CPF and PCF showed with no observable changes in the after calcination; an indication that calcination of FLC with the biomasses did not promote any structural modification in the FLC lattice. Similar results have been reported by Olu-Owolabi et al. (2017) and Unuabonah et al. (2013a). Fig. 1*d* show the infra-red spectra peaks between 4000 and 450 cm^{-1} for the pure and calcined clays. The spectra bands around 3440 cm^{-1} have been assigned to –OH groups vibrations lying within the clay sheets, as well as surface –OH groups which form hydrogen bonds with the oxygen of Si–O–Si bonds (Olu-Owolabi et al., 2016a). The band around 1700 cm^{-1} is characteristic of the C=O stretch of carbonyl double bond while the peaks between 1670 and 1615 cm^{-1} have been attributed to amide-I groups. The bands around 1040 cm^{-1} were attributed to Si–O in plane bending vibrations, while the bands around 740 and 566 cm^{-1} were possibly due to Si–O–Si bridging bonds in SiO_2 and Al–OH/Al–O deformations, respectively (Awala and El Jamal, 2011). All three adsorbents showed similar bands except for the band at 1416 cm^{-1} which was common to CPF and PCF; this peak was attributed to –C–N band indicating a possible position of active interaction between the calcined biomass and the FLC clay (Olu-Owolabi et al., 2016a; Rivera-Utrilla and Sanchez-Polo, 2003).

Results of preliminary experiment on the effect of pH on Pb(II), Cu(II) and Cd(II) adsorption (SM Fig. 1) showed that adsorption was pH dependent for FLC and increased steadily with pH until optimum pH value (≈5.5) where the highest adsorption were recorded for the metals. This trend was attributed to the nature and ionization of adsorption surfaces and metals ions in solution which are significantly influenced by solution pH, and this in turn affects the adsorption of metals in solution (Olu-Owolabi et al., 2012). For instance, at pH values less than 3, there is stiff competition between the positively charged ions (metal ions in solution and protons) for the negatively charged adsorption sites. This leads to protonation of negatively charged adsorption sites and/or displacement of the metal ions from the adsorption sites resulting in low surface adsorption. However, as solution pH increased, the competition

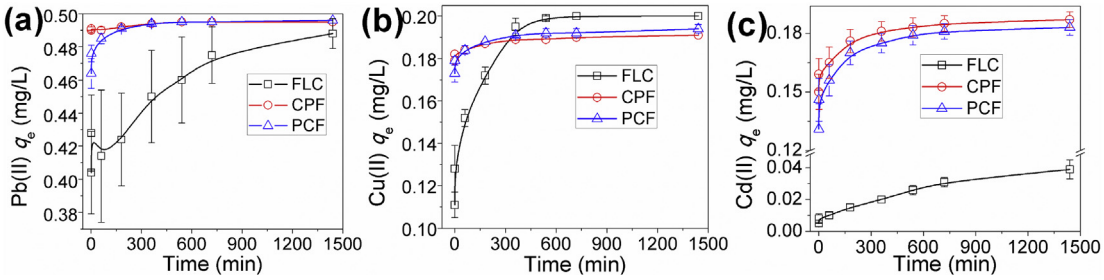

Fig. 2. Effect of time on the adsorption of (a) Pb(II), (b) Cu(II), and (c) Cd(II) ions on FLC, CPF and PCF.

Table 2
Calculated kinetics model parameters for PFOM, PSOM and FPSOM.

		PFOM			PSOM			FPSOM			
		k_1	r^2	*Var*	k_2	r^2	*Var*	k_f	α	r^2	*Var*
FLC	Pb(II)	0.99	0.964	0.0009	0.89	0.984	0.0004	0.15	0.05	0.995	0.0001
	Cu(II)	0.05	0.958	0.40	0.01	0.988	0.11	0.02	0.39	0.998	0.025
	Cd(II)	0.99	0.241	0.24	0.001	0.959	0.013	0.0002	0.48	0.995	0.0016
CPF	Pb(II)	0.99	0.999	1.8×10^{-6}	0.49	0.999	1.8×10^{-6}	1.36	1.94	0.999	3.2×10^{-6}
	Cu(II)	0.20	0.998	0.01	0.13	0.999	0.003	0.63	0.27	0.999	0.00006
	Cd(II)	0.11	0.983	0.11	0.04	0.996	0.024	0.14	0.38	0.999	0.0006
PCF	Pb(II)	0.99	0.996	1.0×10^{-4}	0.50	0.999	1.7×10^{-6}	3.75	0.74	0.999	8.2×10^{-8}
	Cu(II)	0.16	0.996	0.03	0.07	0.999	0.0048	0.26	0.46	0.999	9.3×10^{-5}
	Cd(II)	0.08	0.975	0.15	0.02	0.996	0.024	0.07	0.53	0.999	0.0004

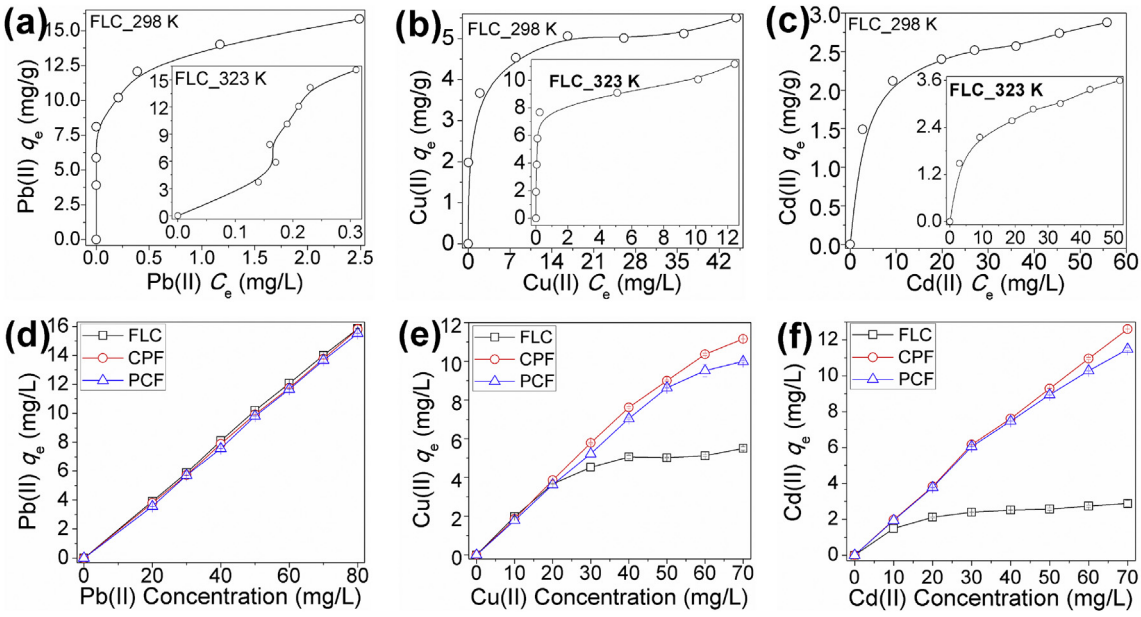

Fig. 3. Adsorption isotherms for (a) Pb(II) (b) Cu(II) (c) Cd(II) on FLC at 298 K (insert: at 323 K); comparisons of the q_e of FLC, CPF and PCF for (d) Pb(II), (e) Cu(II) and (f) Cd(II) adsorption.

reduce steadily due to drop in proton concentration; resulting in gradual increase in adsorption with pH until after optimum pH.

In contrast, adsorption on CPF and PCF were pH independent between pH 3.0 and 6.0. Notwithstanding the higher pHpzc values of the CPF and PCF composites when compared to FLC (≥1.0) (Table 1), adsorption of these cations were significantly below the pHpzc value, an indication of the presence of negatively charged functional groups introduced on the composites' surfaces (Rivera-Utrilla and Sanchez-Polo, 2003). The wide range of pH within which the adsorption capacities of these modified adsorbents are not significantly influenced by the solution pH indicates the versatility of these modified adsorbents in the removal of metal ions from aqueous systems with varied pH.

3.2. Effect of time on adsorption of the metals ions

The effect of time on the adsorption of Pb(II), Cu(II), and Cd(II) were investigated and the results are shown in Fig. 2. It was observed that equilibrium was slower in FLC than in the composites (CPF and PCF) for all three metal ions. Equilibrium was attained for the FLC in 540 min (9 h) for Pb(II) adsorption, while it was faster for Cu(II), 360 min (6 h). Equilibrium for Cd(II) adsorption on FLC was slower and attained in 720 min (12 h). However, for CPF and PCF, equilibria were faster for Pb(II) and Cd(II) adsorption reducing from 540 to 720 min to 60 and 360 min, respectively; while the time was unchanged for Cu(II) adsorption in these composites. The adsorption trend was Pb(II) > Cu(II) > Cd(II); indicating greater affinity for Pb(II) and to a lesser extent Cu(II) than Cd(II) by these adsorbents.

The effects of time on adsorption data were evaluated using the PFOM, PSOM and the homogeneous FPSOM and the various parameters for these models are shown in Table 2 and the plots are shown in SM Fig. 2. Judging with correlation coefficient r^2 and variance (*Var*) values in Table 2, it was observed that the applicability of the models varies with the adsorbent tested. For instance, comparing the simplistic PFOM and PSOM, the PSOM described the data better; implying that the adsorption process was dominated by sharing or exchange of valence electrons between surface sites and metal species which was a fast process dependent more on the availability of adsorption sites rather than metal concentration (Olu-Owolabi et al., 2016b). Comparing the PFOM, PSOM and FPSOM showed that both PSOM and FPSOM gave better r^2 and Var values implying that both models could reasonably describe the adsorption data. However, comparing the PSOM and FPSOM, it was observed that the FPSOM gave more detailed description to the adsorption process. The FPSOM gave the best fits and it also showed that modification increased the rate of metal uptake. The rate constant k_f for the FPSOM model confirmed that the rate of uptake of Pb(II) onto the surfaces of the adsorbents was faster than for Cu(II) and Cd(II) (in the order Pb(II) > Cu(II) > Cd(II)). The same rate (k_2) trend was observed in the PSOM (Table 2) and similarly reported (Diagboya et al., 2015). For the FPSOM, the kinetic parameter (k_f) data shows that the uptake of Pb(II) to the surface of PCF was faster when compared with CPF and FLC (PCF > CPF > FLC) despite the higher surface area of FLC (Table 1). This was attributed to the higher CEC and higher pHpzc values of PCF and CPF. However, the trend was the same for the adsorption of Cu(II) and Cd(II): CPF > PCF > FLC. For the PSOM, there was no significant difference in the rate of adsorption of Pb(II) and Cd(II) to the surfaces of CPF and PCF. However the model suggested a faster rate for the adsorption of Pb(II) onto FLC (k_2 = 0.89). The trend in rate of adsorption was FLC > PCF > CPF for Pb(II), while it was CPF > PCF > FLC for Cu(II) and Cd(II). The PFOM also showed similar rate of uptake of Pb(II) onto the adsorbents, while that for Cu(II) and Cd(II) were CPF > PCF > FLC and FLC > CPF > PCF, respectively. In summary, the relatively low Var and higher r^2 values of the FPSOM indicate the best agreement between the model and the adsorption process, and confirm the model is more accurate for describing the kinetic adsorption data than the classical PFOM and PSOM. The FPSOM suggests a complex adsorption phenomenon of chemical interactions between the metal species and the chemical groups on these adsorbents, and this involves electrostatic interactions, van der Waals, hydrogen bonding, and hydrophobic interactions (Altenor et al., 2009).

3.3. Equilibrium and adsorption isotherm study

The effect of concentration on Pb(II), Cu(II), and Cd(II) adsorption were depicted by the adsorption isotherm curves which were

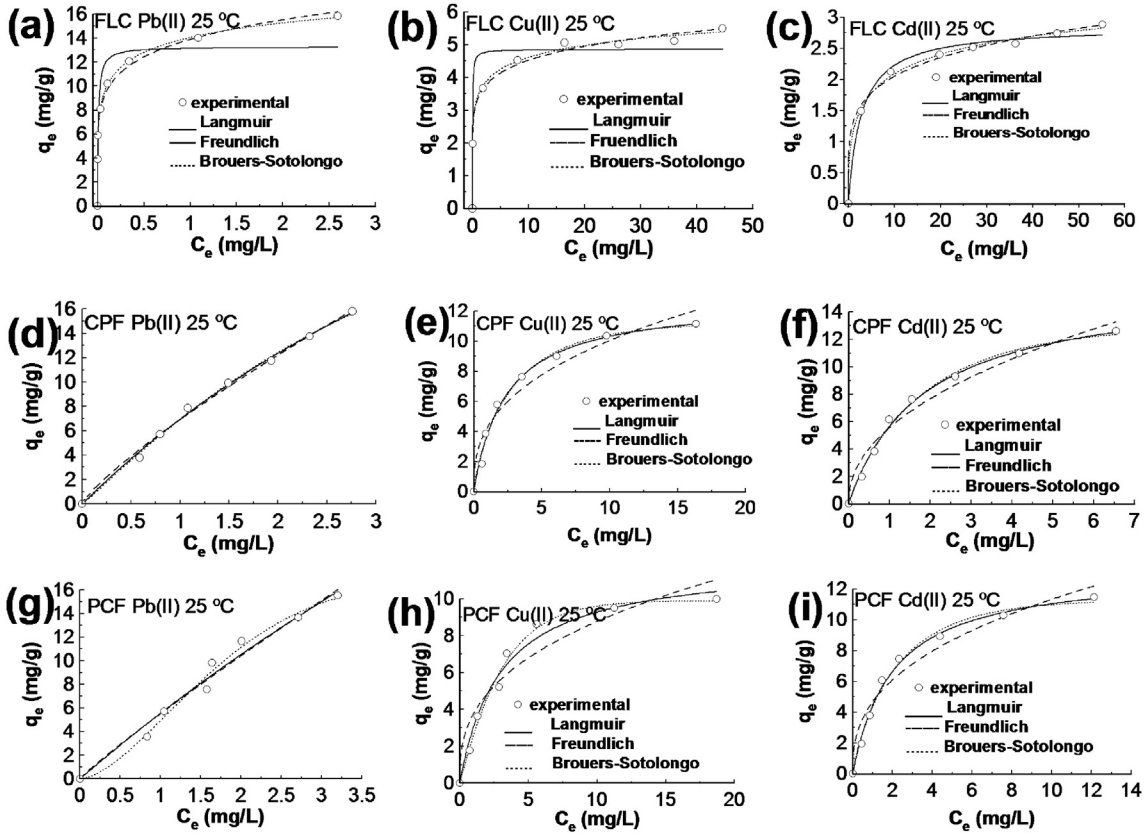

Fig. 4. Experimental plots, Langmuir, Freundlich and Brouers Sotolongo adsorption model plots at 25 °C.

obtained by plotting the q_e vs C_e values (Fig. 3*a-c* and SM Fig. 3). The Figures showed that the curves fit the L type or "Langmuir" isotherms (Giles et al., 1960) for adsorption at 298 K except for Pb(II) adsorption at 323 K. The L type isotherm is usually indicative of molecules adsorbed flat on the surface or sometimes, of vertically oriented adsorbates with particularly strong intermolecular attraction. The initial curvature of the L isotherm showed that as more sites in the adsorbents were filled it became increasingly difficult for a bombarding metal ions to find a vacant site available. Adsorption of Pb(II) at 323 K fitted the *S* type isotherm and the direction of curvature showed that adsorption becomes easier as concentration rises. This may be an indication of a multi-layer adsorption on the initially surface adsorbed Pb(II) ion.

A comparison of the adsorption of each metal by the FLC, CPF and PCF (Fig. 3*d*) showed that there was no significant difference in adsorptions of Pb(II) ions on all three adsorbent species, hence the adsorption trend is FLC ≥ CPF ≥ PCF. However, CPF and PCF showed significant increments (Fig. 3*b* and *f*) in Cu(II) and Cd(II) adsorption; indicating that the composites had higher adsorption capacities for both metals than the pure FLC. The adsorption trends for both Cu(II) and Cd(II) is FLC < PCF < CPF.

The non-linear isotherm curves for the experimental, Langmuir, Freundlich and Brouers–Sotolongo isotherm models are shown in Fig. 4 (and SM Fig. 4). It was observed that the experimental curves rose steeply at low concentration, and quickly approached a plateau at high concentration for all three metals (Fig. 4). The detailed results from the isotherm model fitting are listed in Table 3. It is worthy of note that the closeness of the r^2 values to unity, low *Var.* and the agreement of the Q_o values to the experimentally observed adsorption q_e is a method of determining the adequacy of a model. Hence, considering the r^2, *Var.* and Q_o values obtained by the various adsorption models for these metals and comparing with the experimental data, the Brouers-Sotolongo adsorption isotherm model gave the best fit for these experimental data. This is in line

Table 3
Calculated isotherm model parameters for the Langmuir, Freundlich and Brouers-Sotolongo at 25 °C.

		Langmuir				Freundlich				Brouers-Sotolongo				
		Q_o	b	r^2	*Var.*	k_f	n	r^2	*Var.*	Q_{max}	k_w	α	r^2	*Var.*
FLC	Pb(II)	13.27	106.23	0.8759	4.13	13.90	6.27	0.9948	0.17	20.54	1.15	0.24	0.9993	0.03
	Cu(II)	4.85	25.52	0.9290	0.31	3.37	7.80	0.9944	0.02	7.36	0.63	0.19	0.9965	0.02
	Cd(II)	2.85	0.36	0.9902	0.01	1.30	5.06	0.9953	0.005	3.37	0.42	0.37	0.9973	0.003
CPF	Pb(II)	55.13	0.14	0.9969	0.10	6.93	1.22	0.9954	0.15	26.03	0.31	1.07	0.9970	0.12
	Cu(II)	12.73	0.43	0.9922	0.15	4.27	2.69	0.9546	0.87	11.22	0.41	0.81	0.9897	0.24
	Cd(II)	15.96	0.55	0.9949	0.11	5.56	2.16	0.9697	0.69	12.93	0.57	0.90	0.9934	0.18
PCF	Pb(II)	100.79	0.06	0.9770	0.74	5.52	1.09	0.9747	0.82	17.12	0.34	1.63	0.9869	0.51
	Cu(II)	12.04	0.34	0.9800	0.32	3.77	2.72	0.9196	1.28	9.91	0.30	1.06	0.9899	0.19
	Cd(II)	13.21	0.51	0.9946	0.10	4.68	2.61	0.9572	0.83	11.29	0.49	0.87	0.9919	0.19

Table 4
Thermodynamics parameters for Pb(II), Cu(II), and Cd(II) adsorptions.

		ΔS° (J/mol/K)		ΔH° (kJ/mol)	$-\Delta G^\circ$ (kJ/mol/K)	
		298 K	323 K		298 K	323 K
FLC	Cu(II)	+157.0	+150.9	+11.7	35.1	37.1
	Cd(II)	+162.9	+150.5	+24.0	24.5	24.6
	Pb(II)	+252.4	+233.4	+36.6	38.6	38.8
CPF	Cu(II)	+105.9	+102.5	+6.6	25.0	26.5
	Cd(II)	+122.8	+117.1	+11.0	25.6	26.8
	Pb(II)	+110.6	+105.0	+10.8	22.1	23.2
PCF	Cu(II)	+133.6	+125.6	+15.4	24.4	25.1
	Cd(II)	+128.8	+122.0	+13.0	25.4	26.4

with the FPSOM which suggested a complex adsorption phenomenon of chemical interactions between the metal species and the chemical groups on these adsorbents. This is reasonable taking into account that the starting materials of our adsorbents are from highly heterogeneous. It was also observed that by comparing the r^2, *Var.* and Q_o values, adsorption of Cu(II) and Cd(II) cations onto FLC may also be reasonably explained by both the Langmuir and Freundlich isotherms simultaneously. The Langmuir isotherm model suggests monolayer adsorption on homogeneous surface without interaction between adsorbed species. However, Weber et al. (1992) have shown that when adsorption occurs on dissimilar sites having approximately equal adsorption energies, the sites with similar energies obey the Langmuir adsorption isotherm while a combination of the various Langmuir isotherms within an adsorption system gives close approximation to the Freundlich adsorption isotherm model; hence, the good fit.

Table 3 also showed that the adsorption of Pb(II) ions onto all adsorbents was more favoured than those of Cd(II) and Cu(II) ions. The preference for Pb(II) ions could be best described using the Pearson's hard and soft acids and bases principles (Pearson, 1963; Puls and Bohn, 1988; Unuabonah et al., 2013a). Pb(II) which is a borderline acid is expected to bind to either soft or hard bases while Cd(II) and Cu(II) ions which are soft acids would prefer to interact with soft bases. Since the surface of our adsorbents do contain functionalities such as −COOH and −OH which are hard bases, they would prefer Pb(II) and interact less with Cd(II) and Cu(II) (Puls and Bohn, 1988; Unuabonah et al., 2013a). This preference may also be linked Pb(II) higher first hydrolysis constant, and thus making it more easily hydrolyzed; its higher atomic weight; higher ionic radius, as well as its smaller hydrated radius, making it a better candidate for electrostatic and inner-sphere surface complexation reactions (Usman, 2008).

Considering parameters from other isotherm models used in modeling data obtained in this study, it was observed that modification of FLC with the biomasses did increase the width of the sorption energy distribution on the adsorbent surfaces (α in the Brouers–Sotolongo model) and hence confirming the heterogeneity of the surface adsorption sites (Table 3). Also, change in solution temperature did not significantly this factor, nor did it influence any change in the pattern of these values for the various adsorbents (SM Table 1). The values of n in the Freundlich models, suggest that adsorption of Pb(II), Cd(II) and Cu(II) ions on the various adsorbents follow the L-shaped isotherm pattern (Fig. 3*a-c*; SM Fig. 3) that depicts molecules adsorbed flat on the surface or vertically oriented adsorbates with particularly strong intermolecular attraction (Foo and Hameed, 2010; Badr and Al-Qahtani, 2013).

Table 4 shows the thermodynamic parameters (ΔG°, ΔH°, and ΔS°) obtained for the metals adsorption on all adsorbents. The b values from the Langmuir isotherm model was employed in calculating the thermodynamic parameters. It was observed that the values of enthalpy changes, ΔH°, were positive except for Pb(II) adsorption on PCF. The positive values imply that the reactions were endothermic; hence, increased solution temperature would result in increased uptake of aqueous metal ions (Diagboya et al., 2016). However, modification with biomasses tends to reduce, significantly, the energy requirement for the adsorption process. This is seen in the decrease in the enthalpy of the adsorption reaction.

However, Pb(II) adsorption on PCF was exothermic and higher temperature reduced adsorption. The ΔG° values indicated that the adsorption processes were spontaneous and feasible. The ΔS° values of the adsorptions were positive except for Pb(II) adsorption on PCF, which was negative. This is an indication of increase in randomness of the metal ions at the solid–liquid interface as the adsorption processes proceeded towards equilibrium.

3.4. Reusability study

The regeneration and reusability of the CPF and PCF composites were investigated to evaluate the economic benefits of both composites. Fig. 5 shows the quantities of the metal ions removed initially and upon regeneration and reuse of both adsorbents. It was observed that the second adsorption cycle was slightly lower than the first by approximately 17 and 22% for the CPF and PCF composite adsorbents, respectively. However, the reduction in adsorption capacities observed in the subsequent cycle was far lower than observed in the second cycle: 13 and 5%, respectively. These results suggest that both composite adsorbents may have good regeneration and reusability in wastewater treatment, implying their usefulness economically for water treatment.

4. Conclusion

Feldspar–biomass composites were prepared via calcination of feldspar (FLC) and *Carica papaya* seeds or pine cone seeds to yield

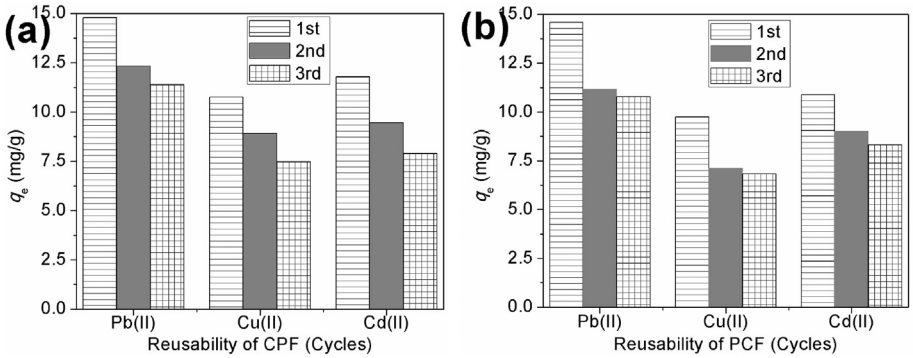

Fig. 5. Reusability of (a) CPF (b) PCF composites for Pb(II), Cu(II), and Cd(II) adsorption.

Carica papaya-FLC (CPF) and pine-cone-FLC (PCF) composite adsorbents, respectively. Physicochemical characterization results indicate that the composite adsorbents, CPF and PCF, exhibited lower specific surface area when compared with the FLC. However, their cation exchange capacities were enhanced; suggesting enhancements in metals' adsorption capacities. Calcination did not promote any structural modification in the basic FLC lattice. Adsorption of Pb(II), Cu(II) and Cd(II) on FLC was pH dependent whereas pH had no observable effect on these metals adsorption on CPF and PCF between pH 3.0 and 6.0. The range of pH within which the adsorption capacities of these adsorbents are not significantly influenced by the solution pH may indicate their versatility in the removal of metal ions from aqueous systems with varied pH. Adsorption equilibria were faster in the composites than in FLC and the rate of Pb(II) uptake was higher than for Cd(II) and Cu(II). Kinetic and equilibrium adsorption isotherm modeling using classical models– pseudo-first order and pseudo-second order kinetic models, Langmuir and Freundlich adsorption isotherm models, as well as the fractal pseudo-second order kinetic model and fractal Brouers–Sotolongo adsorption model showed that the fractal models were best in describing the metals adsorption on the composites. These fractal models suggest a complex adsorption phenomenon of chemical interactions between the metal species and the functional groups on these adsorbents, and this involves electrostatic interactions, van der Waals, hydrogen bonding, and hydrophobic interactions. These adsorption processes were thermodynamically spontaneous, feasible and endothermic; however the modification significantly reduced the energy requirements of the processes. The Brouers–Sotolongo model showed that modification of FLC increased the width of the sorption energy distribution on the composites indicating the heterogeneity of the surface adsorption sites. Hence, metals adsorption on these novel efficient clay-biomass composites could better be described by the fractal adsorption models than the classical ones.

Acknowledgements

We acknowledge the supports of the Alexander von Humboldt Stiftung Foundation Research group linkage Program and the Justus Liebig University, Giessen, Germany where part of the study was carried out.

Appendix A. Supplementary data

Supplementary data related to this article can be found at https://doi.org/10.1016/j.jclepro.2017.10.079.

References

Altenor, S., Carene, B., Emmanuel, E., Lambert, J., Ehrhardt, J.J., Gaspard, S., 2009. Adsorption studies of methylene blue and phenol onto vetiver roots activated carbon prepared by chemical activation. J. Hazard. Mater. 165, 1029–1039.
Awala, H.M., El Jamal, M.M., 2011. Equilibrium and kinetics study of adsorption of some dyes onto feldspar. J. Univ. Chem. Technol. Metall. 46, 221–229.
Badr, N., Al-Qahtani, K.M., 2013. Treatment of wastewater containing arsenic using Rhazya stricta as a new adsorbent. Environ. Monit. Assess. 185, 9669–9681.
Diagboya, P.N., Olu-Owolabi, B.I., Adebowale, K.O., 2015. Effects of aging, soil organic matter, and iron oxides on the relative retention of lead, cadmium, and copper on soils. Environ. Sci. Pollut. Res. 22, 10331–10339.
Diagboya, P.N., Olu-Owolabi, B.I., Adebowale, K.O., 2016. Distribution and interactions of pentachlorophenol in soils: the roles of soil iron oxides and organic matter. J. Contam. Hydrol. 191, 99–106.
Foo, K.Y., Hameed, B.H., 2010. Insights into the modeling of adsorption isotherm systems. Chem. Eng. J. 156, 2–10.
Freundlich, H.M.F., 1906. Über die adsorption in lösungen. Z. Phys. Chem. 57A, 385–470.
Gaspard, S., Altenor, S., Passe-Coutrin, N., Ouensanga, A., Brouers, F., 2006. Parameters from a new kinetic equation to evaluate activated carbons efficiency for water treatment. Water Res. 40, 3467–3477.
Giles, C.H., MacEwan, T.H., Nakhwa, S.N., Smith, D., 1960. Studies in Adsorption. Part XI. A system of classification of solution adsorption isotherms and its use in diagnosis of adsorption mechanisms and in measurement of specific surface areas of solids. J. Soc. Dye. Colour. 74, 3973–3993.
Gregg, S.J., Sing, K.S.W., 1967. Adsorption, Surface Area and Porosity. Academic, New York, p. 208.
Haerifar, M., Azizian, S., 2014. Fractal-like kinetics for adsorption on heterogeneous solid surfaces. J. Phys. Chem. C 118, 1129–1134.
Lagergren, S., 1898. Zur theorie der sogenannten adsorption gelöster stoffe, vol. 24. Kungliga Svenska Vetenskapsakademiens. Handlingar, pp. 1–39.
Langmuir, I., 1916. The constitution and fundamental properties of solids and liquids. J. Am. Chem. Soc. 38, 2221–2295.
Milonjic, S.K.A., 2007. Consideration of the correct calculation of thermodynamic parameters of adsorption. J. Serb. Chem. Soc. 72, 1363–1367.
Mokwenye, I.I., Diagboya, P.N., Olu-Owolabi, B.I., Anigbogu, I.O., Owamah, H.I., 2016. Immobilization of toxic metal cations on goethite-amended soils. J. Appl. Sci. Environ. Manag. 20, 436–443.
Okoli, P.C., Diagboya, P.N., Anigbogu, I.O., Olu-Owolabi, B.I., Adebowale, K.O., 2017. Competitive biosorption of Pb^{2+} and Cd^{2+} ions from aqueous solutions using chemically modified moss biomass (*Barbula lambarenensis*). Environ. Earth Sci. 76, 33.
Olu-Owolabi, B.I., Diagboya, P.N., Ebaddan, W.C., 2012. Mechanism of Pb(II) removal from aqueous solution using a nonliving moss biomass. Chem. Eng. J. 195–196, 270–275.
Olu-Owolabi, B.I., Alabi, A.H., Unuabonah, E.I., Diagboya, P.N., Böhm, L., Düring, R.-A., 2016a. Calcined biomass-modified bentonite clay for removal of aqueous metal ions. J. Environ. Chem. Eng. 4, 1376–1382.
Olu-Owolabi, B.I., Diagboya, P.N., Okoli, C.P., Adebowale, K.O., 2016b. Sorption behaviour of pentachlorophenol in sub-Saharan tropical soils: soil types sorption dynamics. Environ. Earth Sci. 75, 1494.
Olu-Owolabi, B.I., Alabi, A.H., Diagboya, P.N., Unuabonah, E.I., Düring, R.-A., 2017. Adsorptive removal of 2,4,6-trichlorophenol in aqueous solution using calcined kaolinite-biomass composites. J. Environ. Manag. 192C, 94–99.
Pearson, R.G., 1963. Hard and soft acids and bases. J. Am. Chem. Soc. 85, 3533–3539.
Puls, W.R., Bohn, H.L., 1988. Sorption of cadmium, nickel, and zinc by kaolinite and montmorillonite suspensions. Soil Sci. Soc. Am. J. 52, 1289–1292.
Rivera-Utrilla, J., Sanchez-Polo, M., 2003. Adsorption of Cr(III) on ozonised activated carbon. Importance of Cπ-cation interactions. Water Res. 37, 3335–3340.
Unuabonah, E.I., Gunter, C., Weber, J., Lubahn, S., Taubert, A., 2013a. Hybrid clay: a new highly efficient adsorbent for water treatment. ACS Sustain. Chem. Eng. 1, 966–973.
Unuabonah, E.I., Olu-Owolabi, B.I., Taubert, A., Omolehin, E.B., Adebowale, K.O., 2013b. SAPK: a novel composite resin for water treatment with very high Zn^{2+}, Cd^{2+}, and Pb^{2+} adsorption capacity. Ind. Eng. Chem. Res. 52, 578–585.
Usman, A.R., 2008. The relative adsorption selectivities of Pb, Cu, Zn, Cd and Ni by soils developed on shale in New Valley, Egypt. Geoderma 144, 334–343.
Weber Jr., W.J., McGinley, P.M., Katz, L.E., 1992. A distributed reactivity model for sorption by soils and sediments: 1. Conceptual basis and equilibrium assessments. Environ. Sci. Technol. 26, 1955–1962.